

Density-Dependent Isotropic Raman Line Shapes in Compressed Room-Temperature Nitrogen[†]

K. F. Everitt, C. P. Lawrence, and J. L. Skinner*

Theoretical Chemistry Institute and Department of Chemistry, University of Wisconsin, Madison, Wisconsin 53706

Received: December 19, 2003; In Final Form: March 17, 2004

Using the model developed previously by Everitt and Skinner [*J. Chem. Phys.* **2001**, *115*, 8531], we calculate Raman line shapes of nitrogen at room temperature, from the dilute gas limit to over four times the critical density. At low density, it is necessary to use the full Kubo line shape formula, rather than its motionally narrowed limit. Our results for the average frequency shift from the gas phase, the peak frequency shift, and the line width are all in excellent agreement with experiment over the entire density range. The calculations shed some light on the competing physical mechanisms that are responsible for the interesting nonmonotonic density dependences of both the shift and width.

I. Introduction

The isotropic Raman line shape of a neat fluid is a useful probe of structure and dynamics. The shift of the line from its gas-phase value provides information about intermolecular interactions and structure. The width of the line is determined by the distribution of vibrational frequencies in the fluid and the time scale for the frequency fluctuations. As such, a good deal of effort has been expended toward a theoretical understanding of the molecular dynamics and interactions that lead to these frequency fluctuations.^{1–3}

The isotropic Raman line shape for nitrogen has been measured experimentally by many groups, exploring different liquid and supercritical fluid regions of the phase diagram. For example, Oksengorn et al.^{4,5} have measured the line width and shift below the critical temperature, when the system is in the liquid phase. Clouter et al.^{6,7} measured spectra along the coexistence line from the triple point to the critical point, and a few years later, they examined the behavior of the line shape as the critical point is approached from above at constant density.⁸ Musso et al.⁹ performed similar measurements of the line shift and width, which are characterized by phenomenal precision of the temperature near the critical point. Others^{10–15} have performed line shift and width measurements at a constant temperature of 295 K (the critical temperature is 126.2 K) as a function of density, from the dilute limit to over four times the critical density. These experimental results show a number of intriguing features. As the density is increased, the rotationally inhomogeneous isolated-molecule Q-branch structure is first slightly broadened due to intermolecular interactions and then narrowed due to collisions. Eventually, the motionally narrowed limit is reached, even as the line width increases again. The line shift is initially to the red, from intramolecular vibration–rotation coupling, then red-shifts further as the density is increased, finally blue-shifting at higher densities. The interesting nonmonotonic density dependences of both the line width and shift result from competing intramolecular and intermolecular interactions.

There have been a number of theoretical calculations of the isotropic Raman line shape of nitrogen over the past 25 years.^{14–31} The pioneering paper in the field is due to Oxtoby,¹⁶ who showed that one could calculate the line width from a classical molecular dynamics simulation. They considered liquid nitrogen near the normal boiling point (77 K), showed that the line shape is motionally narrowed, and found a line width in quite good agreement with experiment. This calculation included several contributions to a molecule's fluctuating frequency: from the force exerted on the molecular bond by neighbors in the liquid, from the derivative of this force, and from resonant intermolecular vibrational interactions. In a subsequent paper, Levesque et al.¹⁷ also included terms due to vibration–rotation coupling and to changes in the dispersion interaction when the molecule is vibrationally excited. They found that these terms were necessary to get the correct sign of the frequency shift (a red shift at this state point), in agreement with subsequent general arguments put forth by de Souza et al.,³² but did not obtain good agreement with experiment. Gayathri and Bagchi¹⁸ used the model and approach of Oxtoby et al.¹⁶ to calculate the line width along the liquid–gas coexistence line and along the critical isochore, finding reasonable agreement with experiment.

Michels et al.¹⁹ have also calculated the Raman line shape for nitrogen using molecular dynamics simulations. They included all of the contributions described above except those due to resonant intermolecular interactions, and incorporated changes in the dispersion and repulsive interactions upon vibrational excitation through the use of two adjustable parameters. Their room-temperature results were obtained assuming that the line shape is in the motionally narrowed limit and thus are restricted to relatively high densities (higher than twice the critical density). Their results for the width and shift are in good agreement with the room-temperature experiments at these higher densities. Recently, the same group calculated spectra using the full Kubo line-shape expression³³ (rather than assuming the extreme-narrowing limit) at several different thermodynamic state points and found in some cases modest deviations from the motional-narrowing result.²⁰ They did not consider densities lower than twice the critical density at room temperature.

[†] Part of the special issue "Gerald Small Festschrift".

* To whom correspondence should be addressed.

In a similar vein, two of us (Everitt and Skinner) developed a model for nitrogen with all of the contributions to the frequency fluctuations discussed above, including resonant intermolecular vibrational interactions and vibration–rotation coupling.²¹ The ϵ and σ parameters of the two-site Lennard-Jones model were assumed to vary linearly with the vibrational coordinate, and the coefficients were adjusted to fit experimental data for the line shift along the liquid–gas coexistence curve. It was then shown that one could obtain (again assuming extreme motional narrowing) relatively good agreement with the experimental results for the line width along the coexistence curve. Roychowdhury and Bagchi applied this model to study the Raman line width and shift of nitrogen on both the liquid–gas coexistence curve and the critical isochore, finding reasonable agreement with experiment.^{22,23}

In this paper, we calculate the isotropic Raman line shape of room-temperature nitrogen over a wide range of densities, from the dilute gas to the dense fluid. One goal of this paper is to assess the robustness of the model developed by Everitt and Skinner.²¹ This model was parametrized for the dense liquid (with temperatures from 64 to 123 K), and so it is interesting to determine if it can reproduce the experimental line shift and width at room temperature over the entire density range. We find that it can. A second goal of the paper is an understanding of the physical origins of the interesting nonmonotonic density dependences of both the line shift and width.

II. Theoretical Methods

A description of the general approach used to calculate the Raman line shape has been given previously,¹⁶ as have details of the precise model considered herein.²¹ Here we make a few general remarks, mostly dealing with the nuances of how to treat resonant intermolecular vibrational interactions when one is not in the motionally narrowed limit, and present the expressions we use to calculate the line shape.

The Hamiltonian for the nitrogen fluid can be separated into three terms: that for the system, H_v , the bath, H_b , and the system–bath coupling, V . The quantum-mechanical system Hamiltonian describes the vibrations of the collection of isolated nitrogen molecules. As we are not concerned with excitations of more than one quantum of vibrational energy, the relevant eigenfunctions of H_v will be denoted as $|0\rangle$ when all of the molecules are in their ground vibrational states and $|i\rangle$ when only molecule i is in the first excited state. The energy of the ground state is taken to be 0, and the energy of any of the degenerate excited states is $\hbar\omega_0$. The bath Hamiltonian is treated classically and involves the translations, rotations, and intermolecular interactions of all of the molecules.

Oxtoby et al. showed that within the second-cumulant approximation the normalized isotropic Raman line shape is given by¹⁶

$$I(\omega) = \frac{1}{2\pi} \int_{-\infty}^{\infty} dt e^{i(\omega - \omega_0 - \langle\omega\rangle)t} \exp\left\{-\int_0^t dt' (t - t') C(t')\right\} \quad (1)$$

$C(t)$ is the classical time-correlation function of the time-dependent frequency fluctuations of the i th molecule

$$C(t) = \langle \delta\omega_i(t) \delta\omega_i(0) \rangle \quad (2)$$

where

$$\delta\omega_i(t) = \omega_i(t) - \langle\omega\rangle \quad (3)$$

$\langle\omega\rangle = \langle\omega_i(t)\rangle$ is the average frequency fluctuation (i.e., the

solvent shift) and

$$\hbar\omega_i(t) = V_{ii}(t) - V_{00}(t) + \sum_{j(\neq i)} V_{ij}(t) \quad (4)$$

Thus, the instantaneous frequency shifts come from matrix elements of V between eigenstates of H_v . The difference in the diagonal terms is the fluctuating energy gap, whereas the off-diagonal terms come from resonant intermolecular vibrational interactions. These matrix elements are time-dependent due to the classical Newtonian evolution of the bath degrees of freedom. In what follows, we will characterize our calculated line shapes by the shift of the peak frequency from ω_0 , ω_p , the average frequency shift, $\langle\omega\rangle$, and the fwhm, Γ .

As is well-known, the above second-cumulant result is valid if the fluctuations are Gaussian, or if they are weak. Defining the mean-square fluctuations by $C(0) = \Delta^2$, and the correlation time by $\tau = \int_0^\infty dt C(t)/C(0)$, the weak-coupling limit is equivalent to the condition that $\Delta\tau \ll 1$, in which case the line shape is in the motionally narrowed limit, and $\Gamma = 2\Delta^2\tau$.^{33,34} At high density, the room-temperature nitrogen line shapes are in this limit.¹⁹

At lower densities, as collisions become more infrequent, the correlation time is sufficiently long that $\Delta\tau$ is not small compared to 1. Furthermore, the frequency fluctuations are not Gaussian (see below), and so it is not appropriate to use the above second-cumulant result. In this same (low-density) situation, however, resonance transfer terms are not important, and so the frequency fluctuations arise from energy gap fluctuations alone. In this case, a more general semiclassical result for the line shape is^{33,35–37}

$$I(\omega) = \frac{1}{2\pi} \int_{-\infty}^{\infty} dt e^{i(\omega - \omega_0 - \langle\omega\rangle)t} \langle \exp[-i \int_0^t dt' \delta\omega_i(t')] \rangle \quad (5)$$

In the inhomogeneous limit, when the *dynamics* of the frequency fluctuations can be neglected, then this reduces to

$$I(\omega) = \langle \delta(\omega - \omega_0 - \omega_i) \rangle = P(\omega) \quad (6)$$

which as indicated is simply the distribution of vibrational frequencies, $P(\omega)$.

It is convenient and desirable to have a line-shape formula we can use from the zero-density limit (the dilute gas) all of the way to the dense fluid. For low densities, as discussed above, resonant intermolecular vibrational interactions are not important, but non-Gaussian inhomogeneous broadening (due to vibration–rotation coupling) is. Therefore, we use eq 5 for the line shape (with eq 4 for the frequency fluctuations), even though eq 5 is not correct with resonance transfer terms included, because in this limit these terms are negligible. At higher densities, the line shape becomes motionally narrowed, and the resonance transfer terms contribute significantly.²¹ Here again, we use eqs 4 and 5, because in the motionally narrowed (weak-coupling) limit the latter reduces to eq 1, which is valid with resonance transfer terms included.^{16,21} In summary then, we use eq 5 for all densities, with eq 4 for the frequency fluctuations, confident that at least in the low- and high-density limits we make no substantial error.

Finally, we observe that in the zero-density limit all of the frequency fluctuations are static and (as mentioned above) come from (intramolecular) vibration–rotation coupling. In fact, from ref 21, we see that $\omega_i = \xi L_i^2$ (where L_i is the magnitude of the angular momentum of the i th molecule) and

$$\xi = \frac{1}{\hbar I} \left(\frac{3[(q^2)_{11} - (q^2)_{00}]}{2r_e^2} - \frac{[q_{11} - q_{00}]}{r_e} \right) \quad (7)$$

where I is the moment of inertia of the molecules, the matrix elements of the vibrational coordinates are between eigenstates of the isolated-molecule Hamiltonian, and r_e is the bond length. Thus, in this limit, the line shape is given by eq 6, where the average is over a thermal distribution of angular momenta. The result is

$$I(\omega) = P(\omega) = \frac{e^{-(\omega_0 - \omega)/\gamma}}{\gamma}, \quad \omega < \omega_0 \quad (8)$$

with $\gamma = 2IkT|\xi|$. Thus, this exponential distribution is peaked at $\omega = \omega_0$ (and so $\omega_p = 0$), has an average frequency shift of $\langle\omega\rangle = -\gamma$, and has a width of $\Gamma = \gamma \ln 2$. Using the parameters and matrix elements listed in ref 21, at 295 K, $\gamma = 1.71 \text{ cm}^{-1}$.

III. Results and Discussion

Molecular dynamics simulations were performed with 500 rigid nitrogen molecules. The model describing the molecular interactions consisted of two Lennard-Jones sites for each molecule placed at the atomic positions, the parameters of which can be found in ref 21. The equations of motion were integrated using a leapfrog algorithm with an integration time step of 4 fs.³⁸ All of the simulations were performed at room temperature (295 K), but over a wide span of densities, ranging from the dilute gas to a dense fluid. From a simulation, the fluctuating frequency of each molecule can be calculated as a sum of kinetic and potential energy contributions from eq 4 (again, the details may be found in ref 21). From the simulation results, we then calculate statistically meaningful quantities such as the average frequency, $\langle\omega\rangle$, the frequency time-correlation function, $C(t)$, and the line shape, $I(\omega)$.

In Figure 1, we show the calculated line shapes and frequency distributions as a function of density (for $T = 295 \text{ K}$), from the isolated molecule up to twice the critical density (for nitrogen, $\rho_c = 6.73 \text{ nm}^{-3}$). Note that to facilitate comparison, these line shapes and distributions have been scaled so as to have the same peak height. At $\rho = 0$, the line shape and the frequency distribution are identical and are obtained not from a simulation but rather from eq 8. As the density increases and molecular interactions become important, the frequency distributions (now calculated from the simulation) shift to the red, broaden, and become more symmetrical. The line shapes also shift to the red (of course) and become more symmetrical and show substantial motional narrowing (in that the line shapes are narrower than the distributions). By $\rho = 2\rho_c$, the line shape is nearly Lorentzian.

As mentioned earlier, we characterize the line shapes by $\langle\omega\rangle$, ω_p , and Γ , and these are shown as a function of density in Figure 2. In the upper panel, we compare the average frequency shift $\langle\omega\rangle$ and peak frequency shift ω_p of the line shape. One sees that at low density these can be quite different, since the line shapes are asymmetrical, but that by about twice the critical density the line shape is symmetrical, and so the average and the peak are the same. In the lower panel, we plot the line width as a function of density. Except at very low densities (which is obscured in this figure, but see below), the line width decreases monotonically until about $\rho = 2.5 \rho_c$, at which point it starts increasing. It is also interesting to compare this to the fwhm of the frequency distributions, as shown in the figure as the solid squares. At $\rho = 0$, of course they are the same, but as density increases, the line width becomes substantially smaller than the

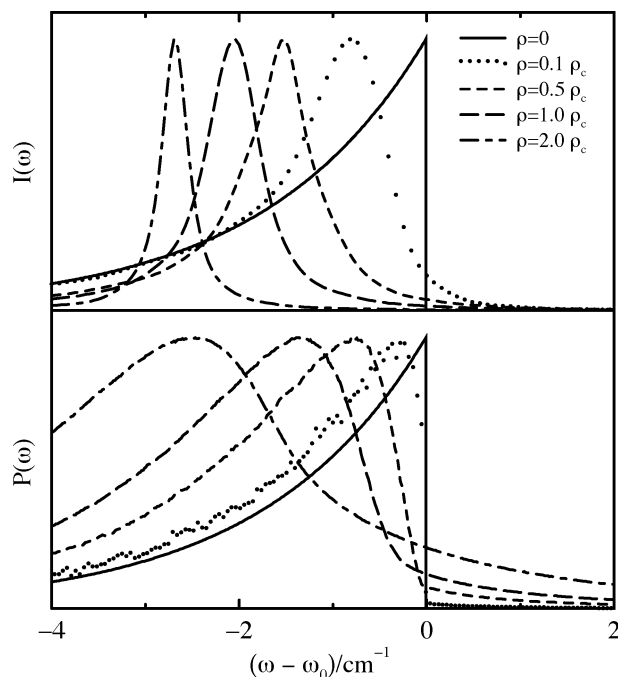


Figure 1. Line shapes, $I(\omega)$, and frequency distributions, $P(\omega)$, at 295 K for several different densities.

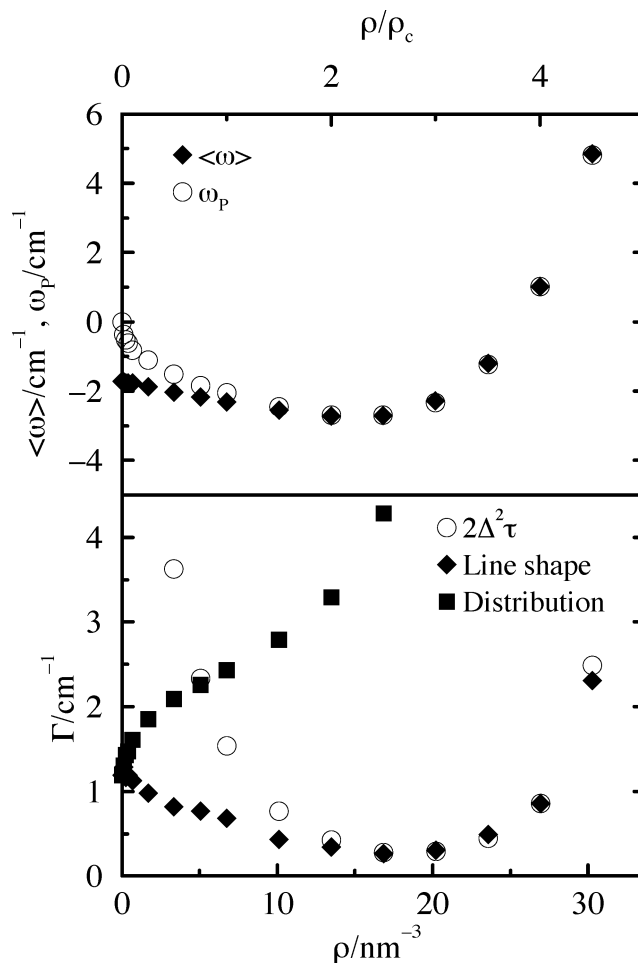


Figure 2. Average frequency shift, $\langle\omega\rangle$, peak frequency shift, ω_p , and line width, Γ , at 295 K as a function of density. Also shown are the width of the frequency distribution and the line width in the motionally narrowed limit, $2\Delta^2\tau$.

width of the distribution due to motional narrowing. Finally, in the figure, we also show the results from $\Gamma = 2\Delta^2\tau$ (Δ and τ

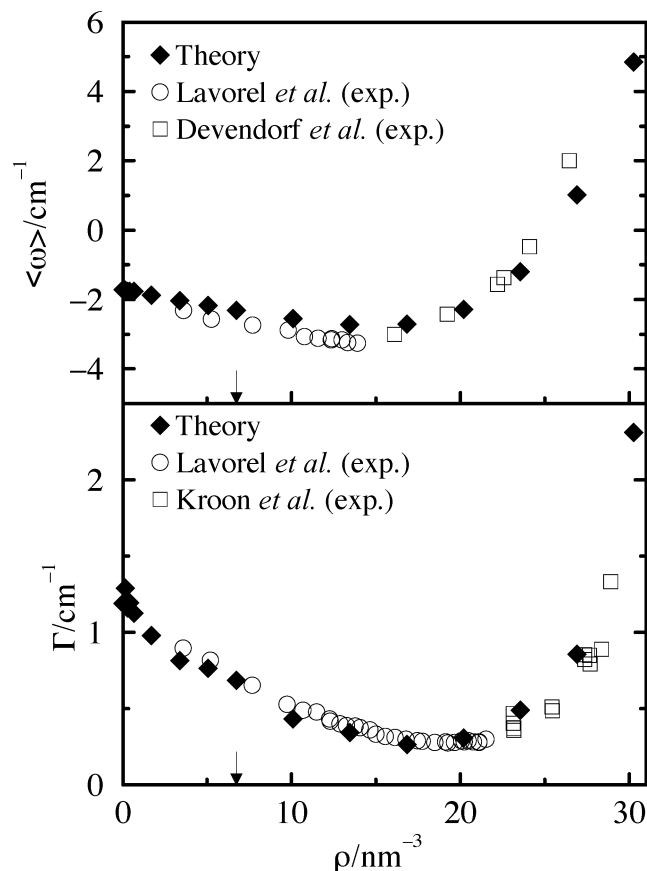


Figure 3. Average frequency shift, $\langle\omega\rangle$, and line width, Γ , as a function of density: comparison of theory with experiment. The arrows show the critical density.

are calculated from the simulation). We see that for ρ greater than about 15 nm^{-3} this formula is accurate, showing that in this case the line shape is a motionally narrowed Lorentzian, whereas for smaller densities, it is not.

The physical origin of the nonmonotonic behavior of the line shift is as follows: at zero density, the shift is negative due to the vibration–rotation coupling. As the density increases, this contribution remains constant (as it is a function of temperature only), whereas a number of additional terms become significant, both from the force exerted by neighboring molecules directed along the bond and from polarization effects (modeled by vibrational-coordinate-dependent Lennard-Jones parameters).²¹ To first order, these terms are either proportional to the interaction energies or forces exerted between pairs of molecules.²¹ These contributions are both positive and negative and thereby compete with one another. As it turns out, at relatively low density, these terms result in a larger red shift. However, as the density continues to increase, the fluid becomes tightly packed and the molecules ride up the repulsive wall of the intermolecular potential. The net result is that these terms due to the intermolecular interactions change sign and become larger. Thus, one observes a rapidly increasing frequency shift toward the blue.

The density dependence of the line width is actually considerably easier to understand. At zero density, the system is in the inhomogeneous limit and the width is determined by the distribution of frequencies, caused by the thermal distribution of rotational energies. As the density increases and the intermolecular interactions become important, variations in the distances between molecules cause the width of the frequency distribution to increase. However, despite this increase, motional

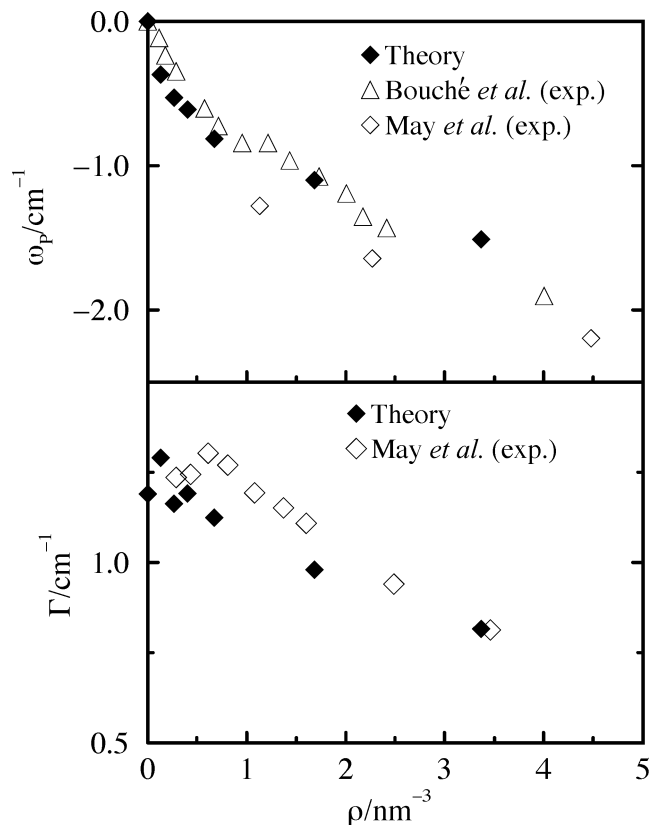


Figure 4. Peak frequency shift, ω_p , and line width, Γ , as a function of density for low densities: comparison of theory with experiment.

narrowing quickly becomes important and the line width decreases as the correlation time τ decreases due to collisions. As the density increases further, the correlation time stops decreasing (that is, it becomes relatively insensitive to density), and so the line width now increases as the width of the distribution of frequencies continues to rise.

In Figure 3, we compare the values we obtained for the average frequency shift and line width to the experimental results over the full range of densities.^{10,11,14} For both the shift and width, we find excellent agreement with experiment. This is quite rewarding since in our original treatment of low-temperature nitrogen line shapes we used the experimental data for the frequency shift along the gas–liquid coexistence curve to fit the parameters of our model.²¹ Using these parameters, we then compared our calculated line widths to experiment (again along the coexistence curve) and found reasonable agreement. Our present results at this high temperature (without any further adjustment of parameters) show that the model we developed is robust in that it is able to treat accurately state points far from those used in our original fit.

Finally, we make two other points about the line shape for low densities. First, at zero density, the *experimental* line shape does not actually decrease monotonically to the red as in Figure 1 but rather has structure due to individual rotational quantum states.^{12,31,39} This structure is of course not captured in our model (where the rotations are classical), but the envelope of the experimental Q-branch is given quite well by our model. Furthermore, at low but finite density, the rotational structure is washed out experimentally, and so our classical model is adequate. Second, it is interesting to examine more closely the behavior of the line width and shift at low density. Figure 4 shows our calculated peak frequency shift, compared to the corresponding experimental^{12,13} results at low density, and also the theoretical and experimental¹³ line widths. One sees that

for the shift the agreement between theory and experiment is excellent. Although the agreement for the width is not quite quantitative, it is particularly fascinating that the slight increase in the experimental width at very low density is captured by the theory. This increase is due to an initial broadening of the distribution of frequencies as density is increased before there is significant motional narrowing.

IV. Conclusions

In this work, we calculated isotropic Raman line shapes for nitrogen at room temperature over a wide range of densities from 0 to over 4 times the critical density, using the usual semiclassical Kubo line shape formula. At low density, the line shape is inhomogeneously broadened due to a thermal distribution of rotational energies, whereas at higher density, the line shape becomes motionally narrowed. Both the average frequency shift and the line width have nonmonotonic density dependences, which result from competing intramolecular (vibration-rotation) and intermolecular interactions, as described above. Experimental results for the average frequency shift, the peak frequency shift, and the line width are all in excellent agreement with theory over the entire range of densities. Even the subtle initial increase of the line width at low density is produced by the theory. Thus, the model developed by Everitt and Skinner,²¹ which was parametrized from experimental data along the coexistence line (with temperatures from 64 to 123 K), is robust enough to produce accurate results at room temperature.

Acknowledgment. J.L.S. is delighted to dedicate this paper to Gerry Small, who has been a good friend and colleague for over twenty years. The authors are grateful for support from the National Science Foundation (Grant No. CHE-0132538).

References and Notes

- (1) Oxtoby, D. W. *Adv. Chem. Phys.* **1979**, 40, 1.
- (2) Oxtoby, D. W. *J. Phys. Chem.* **1983**, 87, 3028.
- (3) Schweizer, K. S.; Chandler, D. *J. Chem. Phys.* **1982**, 76, 2296.
- (4) Oksengorn, B.; Fabre, D.; Lavorel, B.; Saint-Loup, R.; Berger, H. *Chem. Phys. Lett.* **1989**, 164, 23.
- (5) Oksengorn, B. *J. Chem. Phys.* **1991**, 94, 1774.
- (6) Clouter, M. J.; Kiefte, H. *J. Chem. Phys.* **1977**, 66, 1736.
- (7) Clouter, M. J.; Kiefte, H.; Jain, R. K. *J. Chem. Phys.* **1980**, 73, 673.
- (8) Clouter, M. J.; Kiefte, H. *Phys. Rev. Lett.* **1984**, 52, 763; Clouter, M. J.; Kiefte, H.; Deacon, C. G. *Phys. Rev. A* **1986**, 33, 2749.
- (9) Musso, M.; Matthai, F.; Keutel, D.; Oehme, K.-L. *J. Chem. Phys.* **2002**, 116, 8015.
- (10) Lavorel, B.; Oksengorn, B.; Fabre, D.; Saint-Loup, R.; Berger, H. *Mol. Phys.* **1992**, 75, 397.
- (11) Kroon, R.; Baggen, M.; Lagendijk, A. *J. Chem. Phys.* **1989**, 91, 74.
- (12) Bouché, T.; Dreier, T.; Lange, B.; Wolfrum, J.; Franck, E. U.; Schilling, W. *Appl. Phys. B* **1990**, 50, 527.
- (13) May, A. D.; Stryland, J. C.; Varghese, G. *Can. J. Phys.* **1970**, 48, 2331.
- (14) Devendorf, G. S.; Ben-Amotz, D. *J. Phys. Chem.* **1993**, 97, 2307.
- (15) Meléndez-Pagán, Y.; Ben-Amotz, D. *J. Phys. Chem. B* **2000**, 104, 7858.
- (16) Oxtoby, D. W.; Levesque, D.; Weis, J.-J. *J. Chem. Phys.* **1978**, 68, 5528.
- (17) Levesque, D.; Weis, J.-J.; Oxtoby, D. W. *J. Chem. Phys.* **1980**, 72, 2744.
- (18) Gayathri, N.; Bagchi, B. *Phys. Rev. Lett.* **1999**, 82, 4851.
- (19) Michels, J. P. J.; Scheerboom, M. I. M.; Schouten, J. A. *J. Chem. Phys.* **1995**, 103, 8338.
- (20) Kooi, M. E.; Smit, F.; Michels, J. P. J.; Schouten, J. A. *J. Chem. Phys.* **2000**, 112, 1395.
- (21) Everitt, K. F.; Skinner, J. L. *J. Chem. Phys.* **2001**, 115, 8531.
- (22) Roychowdhury, S.; Bagchi, B. *Phys. Rev. Lett.* **2003**, 90, 075701.
- (23) Roychowdhury, S.; Bagchi, B. *J. Chem. Phys.* **2003**, 119, 3278.
- (24) Hills, B. P.; Madden, P. A. *Mol. Phys.* **1979**, 37, 937.
- (25) Mukamel, S.; Stern, P. S.; Ronis, D. *Phys. Rev. Lett.* **1983**, 50, 590.
- (26) Temkin, S. I.; Burshtein, A. I. *Chem. Phys. Lett.* **1979**, 66, 57.
- (27) Temkin, S. I.; Steele, W. A. *Chem. Phys. Lett.* **1993**, 215, 285.
- (28) Temkin, S. I.; Steele, W. A. *J. Phys. Chem.* **1996**, 100, 1996.
- (29) Strekalov, M. L.; Burshtein, A. I. *Chem. Phys.* **1983**, 82, 11.
- (30) Strekalov, M. L. *Chem. Phys.* **1997**, 222, 223.
- (31) Dreier, T.; Schiff, G.; Suvernev, A. A. *J. Chem. Phys.* **1994**, 100, 6275.
- (32) de Souza, L. E. S.; Guerin, C. B. E.; Ben-Amotz, D.; Szeleifer, I. *J. Chem. Phys.* **1993**, 99, 9954.
- (33) Kubo, R. *Adv. Chem. Phys.* **1969**, 15, 101.
- (34) Schmidt, J. R.; Sundlass, N.; Skinner, J. L. *Chem. Phys. Lett.* **2003**, 378, 559.
- (35) Saven, J. G.; Skinner, J. L. *J. Chem. Phys.* **1993**, 99, 4391.
- (36) Mukamel, S. *Principles of Nonlinear Optical Spectroscopy*; Oxford University Press: New York, 1995.
- (37) Stephens, M. D.; Saven, J. G.; Skinner, J. L. *J. Chem. Phys.* **1997**, 106, 2129.
- (38) Allen, M. P.; Tildesley, D. J. *Computer Simulation of Liquids*; Clarendon Press: Oxford, U.K., 1987.
- (39) Rolland, P.; Pouligny, B.; Morin, E.; Menil, A.; Dejean, J. P. *Mol. Phys.* **1994**, 81, 31.